

Studies on Heterostructure of Bi-2212 and MgB₂ Superconductors

M. Padmavathi,^{1*} Putha Kishore²

¹Department of Physics, SKR&SKR Govt. Degree College for Women (A), Kadapa, AP 516001, India. ²Department of H & S (Physics), KSRM College of Engineering, Kadapa, AP 516005, India.

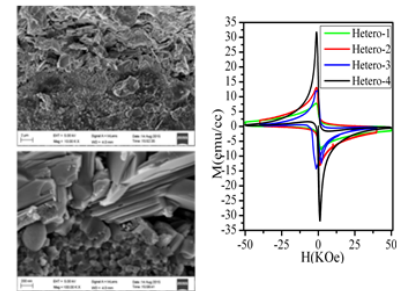
Received on: 21-Jul-2022, Accepted and Published on: 14-Oct-2022

ABSTRACT

Systematic studies on the heterostructure of Bi-2212 and MgB₂ superconductors are reported. Bulk multilayer superconductors are prepared as Bi-2212-MgB₂-Bi-2212 with varying thicknesses of the MgB₂ layer. X-ray diffraction and DC magnetization characterization investigations confirmed the existence of both superconducting phases in heterostructured samples. The morphology of the samples at the surface and in cross section shows that the well crystallised grains of superconducting phases. The critical current density has increased in multilayers of Bi-2212 and MgB₂ superconductors owing to an increase in the superconducting volume fraction. In a tri-layer sample, inverted anisotropy in J_c is observed owing to the improvement of ab -plane properties because of the multilayer growth process. The instability of J_c at high field is observed due to various pinning mechanisms and microstructural changes in the samples.

Bi-2212 and MgB₂
Multilayered
Superconductor

Synthesis



Keywords: High Superconductors, Bulk multi layers, DC Magnetization, Critical current density, Surface Morphology, Pinning mechanism

INTRODUCTION

The heterostructure of the superconductor with the metal, the insulating semiconductors, and the superconductor has been investigated in recent years. The heterostructure of both superconductors is very interesting for their present and future applications. The structural and chemical compatibility between the oxide matrix and the pinning phase allows a powerful vortex pinning and opens the opportunity for growth of superconducting super lattice structures. The multilayer growth method enhances the possibility of high field applications with a high critical current density (J_c) in all configurations. Anisotropy in J_c , defined as the ratio of J_c parallel to the ab plane (J_c^{ab}) and J_c parallel to the c -axis (J_c^c), decreased in artificially engineered super lattices of pnictides¹ and YBCO.^{2,3} The high T_c BiSCCO-2212 superconductor has a

complicated unit cell structure, in which some atoms are oxygen-poor perovskite-like structures, while others appear to be rock-salt structures. In the perovskites and associated compounds, there are a variety of physical properties that make this family an excellent candidate for assembling heterostructures and analysing and exploiting interfacial phenomena. The superconducting super lattices of Bi-2212 with various numbers of Bi-2201 were extensively studied by Eckstein et al.,⁴ and it was concluded that the high- T_c superconductivity is a result of the pairing interaction. The superconducting condensates are essentially two-dimensional, and a small coupling between adjacent high-temperature unit cells is necessary in order to form them.

The super lattices of YBCO and non-superconducting PBCO resulted in a reduced superconductive transition temperature because of parasitic effects in YBCO₅. Compared to a single Nb layer, multilayer growth of NbN on top of an Nb layer enhanced the effective first penetration field of Nb layer.⁶

In this study, the heterostructures of Bi-2212 and MgB₂ superconductors were formed through artificial pinning engineering. At ambient conditions, bulk multi-layers of Bi-2212 and MgB₂ superconductors were prepared through a hydraulic pressure unit. By using hydraulic pressure unit at ambient conditions, bulk multilayered superconductors of Bi-2212 and

Dr. M. Padmavathi, Department of Physics, SKR & SKR GDCW (A), Kadapa, AP, India – 516001.
Tel: +91 6302983846
Email: paddu.manchi@gmail.com

Cite as: *J. Integr. Sci. Technol.*, 2023, 11(1), 437.
URN:NBN:sciencein.jist.2023.v11.437

©Authors CC4-NC-ND, ScienceIN ISSN: 2321-4635
<http://pubs.thesciencein.org/jist>

MgB₂ were prepared. The magnetic and structural properties of the synthesised samples have been given and discussed in detail.

EXPERIMENTAL TECHNIQUES

Here we prepared bi-layer and tri-layer heterostructures of Bi-2212 and MgB₂ layered superconductors. First, Bi-2212 superconductors were prepared through the glass ceramic route as described in reference⁷. The glass ceramics were grinded for one hour using an agate mortar, and then the prepared powder was pressed as a pellet at ambient conditions using a hydraulic pressure unit. On top of that, a pellet of MgB₂ is made at the same pressure, and the thickness of the MgB₂ layer is ~ 0.5 mm, which is named as a Hetero-1 in the series. Another bi-layer sample with an MgB₂ layer having thickness of 0.4 mm is prepared and named as a Hetero-2.

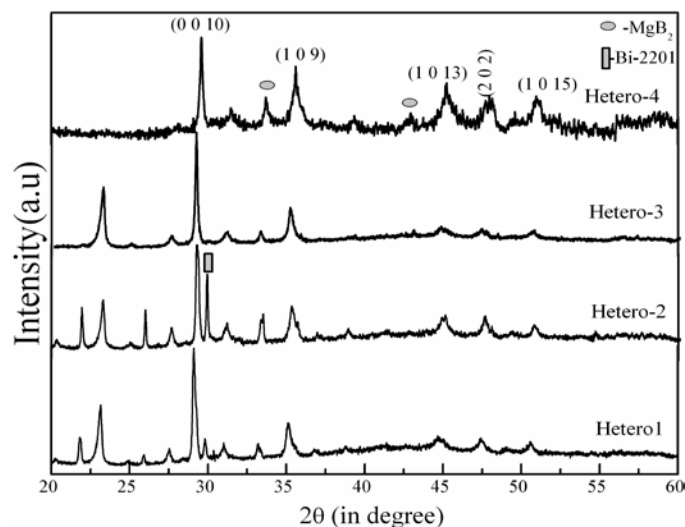


Figure 1 XRD pattern for the various samples.

Further, a tri-layer sample was prepared with Bi-2212 glass-ceramic as the top and bottom layers and MgB₂ as the middle layer. Two tri-layer samples were prepared with varying thicknesses of 0.7 mm and 0.6 mm of MgB₂ layer, and these are called Hetero-3 and Hetero-4 respectively. The crystalline structures of the prepared heterostructures were characterised using the powder X-ray diffractometer (Bruker) with Cu- α radiation. Superconducting phase identification was done by DC magnetization measurement of the samples using the physical property measurement system (PPMS). The surface morphology and phase separation were illustrated by transmission electron microscopy (TEM) and field emission scanning electron microscopy (FESEM). Hysteresis loops for the prepared heterostructures were recorded at 10K using PPMS.

RESULTS AND DISCUSSION

The XRD characterization of the prepared heterostructure samples is shown in figure 1. The peak assignment to the prepared samples was done using JCPDS software. The presence of both Bi-2212 and MgB₂ major phases along with a small amount of Bi-2201 impurity phase is also clearly noticeable in the XRD pattern. Broad

peaks along with satellite peaks at high angles confirm the super lattice structure of the prepared bulk multilayer samples.

The morphology of the samples is observed at the surface and interfaces of the layers through FESEM images of the samples as shown in figures 2 to 5. Figure 2 illustrates the interface of the Hetero-1 sample at different magnifications. From these images, one can observe low porosity and good adherence at the interface of Bi-2212 and MgB₂ layers, and well-crystallized grains were observed in both layers.

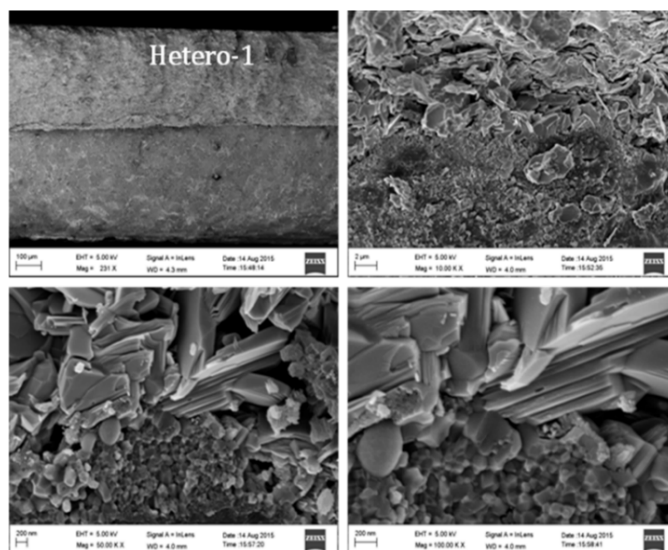


Figure 2 FESEM images for Hetero-1 sample at different scales

Figure 3 shows FESEM images at the interface of a Hetero-2 sample at various magnifications. It is observed from the images that the increase in the porosity at the Hetero-2 sample interface when compared to Hetero-1. Well crystallised spherical grains of MgB₂ and platelet-like structured grains of Bi-2212 are also clearly observed in the images. Figure 4 represents the FESEM images for the Hetero-3 sample, in which three layers are clearly observed, and one of the interfaces is shown at different magnifications.

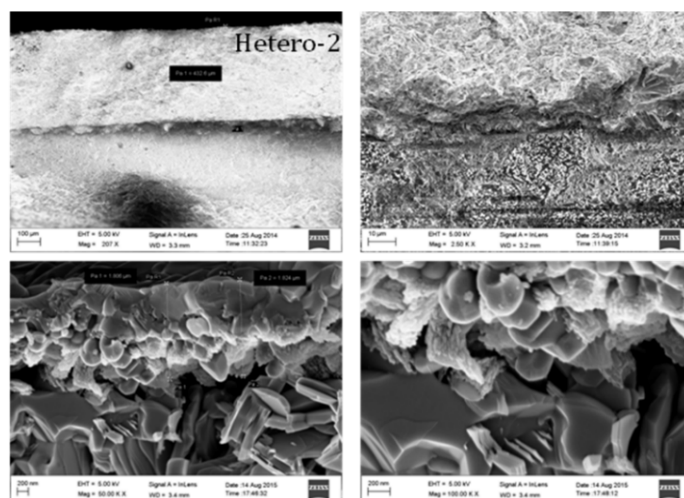


Figure 3 FESEM images for Hetero-2 sample at different scales.

samples. The superconducting transition temperature of heterostructure samples is measured from the magnetization with respect to the temperature data from PPMS. The DC magnetization data of various samples in the zero field cooled (ZFC) and field cooled (FC) processes are shown in Figure 7(a). The FC process was carried out under an applied DC magnetic field of 100 Oe. It is observed that the prepared heterostructures have two transitions, 80 K and 39 K corresponding to Bi-2212 and MgB2 respectively. It shows that as the MgB2 layer thickness decreases, the superconducting volume fraction is increasing. The tri-layer samples have more superconducting volume fraction than the bi-layer samples.

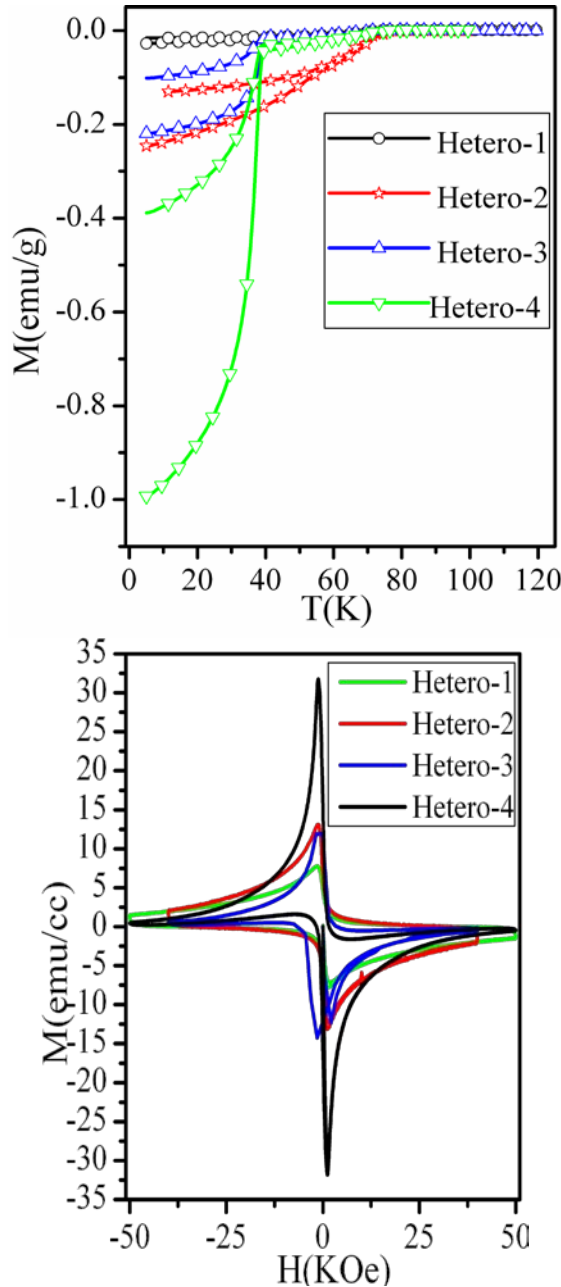


Figure 7(a) Magnetization with respect to the Temperature plots for the samples (b) Magnetization Hysteresis loops at 10K for various samples

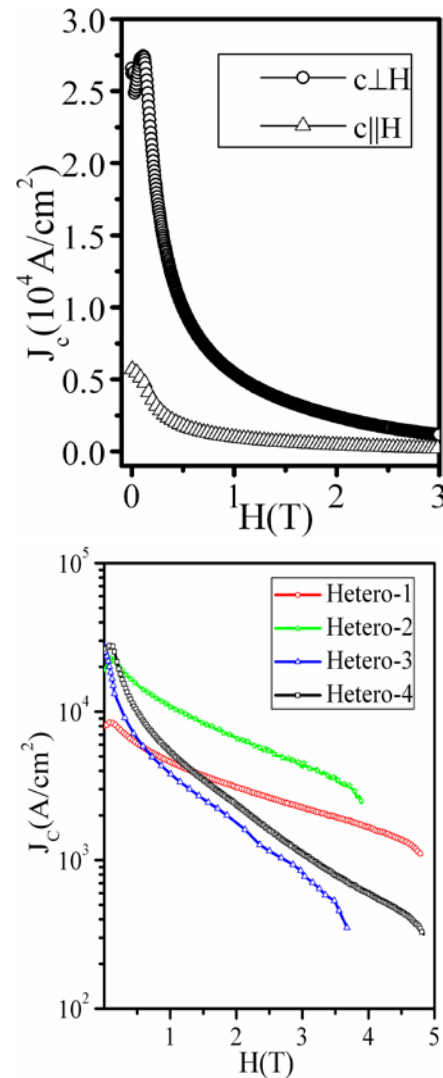


Figure 8(a) J_c anisotropy in Hetero-4, (b) J_c variation with field in the samples.

The magnetic hysteresis loops on the rectangular samples were measured at 10K by applying the field perpendicular to the sample surface as shown in figure 7(b). The hysteresis loops of the samples depict an asymmetric nature, which is an intrinsic property of the Bi-2212 superconductor.⁸ From this, it is observed that the Bi-2212 is dominant in the hetero samples. It is clearly demonstrated by the asymmetric nature as it is increased from bi-layer to tri-layer samples. The magnetic moment also increases considerably. It is well known that the hysteresis loop width is directly proportional to the flux trapped in the superconductor. The same sample can have different $M(H)$ curve shapes at distinct temperatures or up to distinct values of maximal magnetic field. The $M(H)$ can be affected by the geometric structure, shape, and homogeneity of the sample. The high magnetic field in the $M(H)$ curve had a pronounced asymmetry with reference to the $M=0$ axis at temperatures above 10K, and the asymmetric parts of the hysteresis loop are only present in the second and fourth quadrants. This asymmetry is grows with respect to the applied temperature.⁹⁻¹⁶ The

J_c is calculated for all the prepared samples with the help of a magnetic hysteresis loop in the form of a rectangular slab.

The hysteresis loops show trapped flux at low fields and fast flux creeping at high fields (figure 7(b)). By using the Beans extended critical state model, the J_c is measured as given the equation

$$J_c = 20 \left(\frac{\Delta M}{a} \right) \quad (1)$$

Here $d = b [1 - (b/3a)]$, $\Delta M (M^+ - M^-)$ is the width of the M-H loop and a, b are sample dimensions and $a > b$. Figure 8 shows the magnetic field dependence of J_c at 10K for all the heterostructure samples. By plotting in-plane and out-of-plane J_c with applied field, anisotropy in J_c is observed in the Hetero-4 sample (figure 8(a)). Anisotropy in J_c is anticipated as the in-plane critical current density value of J_{cab} , it should be at least 60% higher than the values along the c-axis direction J_{cc} . The J_c anisotropy ratio for aligned MgB2 crystallites at $H=0$ is 1.5.¹⁷ In the case of the (tri-layer) Hetero-4 sample, J_{cc} is higher than J_{cab} and the inverted J_c anisotropy ratio is 4.6 at $H=0$. This high inverted anisotropy in J_c is owing to an increase in ab-plane properties, which may be due to the process of multilayer growth in a tri-layer (Hetero-4) sample. Figure 8(b) shows J_{cc} with respect to the applied field for all the samples.

Figure 8(b) made it abundantly evident that the critical current density of the self-field (J_{czero}) improves from bilayer to tri-layer samples while decreasing the magnetic field of 3Telsa. When compared to a tri-layer sample, a bi-layer sample has a higher J_c . When compared to bi-layer samples, there is a noticeable reduction in J_c for tri-layer samples. When compared to bulk Bi-2212, Figure 8 showed that the J_c is higher in heterostructured samples. In J_c increment, proximity and interfacial effects are two potential outcomes. The absence of a change in T_c for the two superconducting phases in all heterostructured samples eliminates the possibility of proximity transition in these samples. The interfacial effects predominate in the samples due to bulk

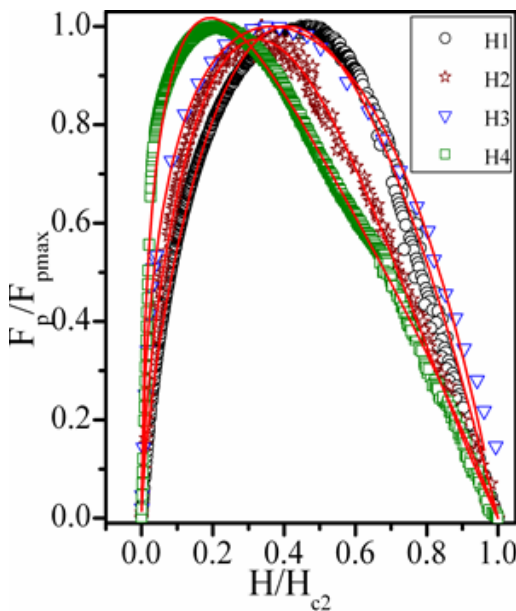


Figure 9. The response of the normalized pinning for reduced magnetic field.

superconducting layers. As a result, the increase in superconducting volume percentage is responsible for the increase in J_c as the layer's thickness increases. When compared to bi-layer samples, tri-layer samples have sharply lower J_c due to structural flaws and unique pinning mechanisms.

Pinning force per unit volume is measured by the following equation

$$F_p = \mu_0 H \times J_c \quad (2)$$

where $\mu_0 = 4\pi \times 10^{-7} \text{N/A}^2$, and found that pinning force is increased in Hetero samples.

The impact of a lower field on the normalised pinning force at 10K is seen in Figure 9. For Hetero-1 through Hetero-4 samples, h_{max} values were found to be 0.5, 0.31, 0.29, and 0.2, respectively. This demonstrates the fact that each heterostructure sample has a unique dominant pinning mechanism. The pinning in the Hetero-1 is mostly caused by volume pinning centres. Similarly, the dominated pinning mechanism in the Hetero-2 and Hetero-3 samples is point, whereas the dominating pinning mechanism in the Hetero-4 sample is surface alone.

Dew Hughes made the following predictions: "Grain, twin and marten site borders, stacking faults, sub-grain dislocations, polygonised boundaries, plate-like precipitates, and the surface of the superconductor behaves like a surface pinning centres. Nano size impurity phases operate as point pinning centres, while large precipitates and thick-walled dislocation cell structures act as volume pinning centres.¹⁸ The Kramer fit to the collected data from all the samples provided strong support for this study. The Kramer fit for the normalised pinning force response to the lowered magnetic field revealed the precise geometry of the pinning centres. The relationship between normalised pinning force and the geometry of pinning centres is given by the Kramer theory¹⁹

$$F(h) = \frac{F_p}{F_{pmax}} = Ah^p(1-h)^q \quad (3)$$

Where h is reduced field defined as H/H_{c2} , p and q are pinning centers shape parameters and A is constant. The values of p and q for various pinning centers are given below table 1.

Table 1 The p and q values for various pinning centers

Pinning	p	q
Point	1	2
Surface	0.5	2
Volume	1	1

The exact pinning geometry in the current samples could not be explained by either the surface pinning, point pinning, or their combined fits. However, by combining all of the pinning processes in the following equation, we were able to successfully fit the curve.

$$F(h) = A_s h^{0.5} (1-h)^2 + B_p h (1-h)^2 + C_v (h(1-h)) \quad (4)$$

This equation gave the best fit for all the samples. It is perceived that the grain boundaries served as surface pinning centers, whereas impurity phases and lattice defects served as point and volume pinning centers. The dominating pinning mechanism is determined from the corresponding fitting constants (A_s , B_p , and C_v for surface, point, and volume pinning respectively), and the obtained values are given in table 2.

Table 2. Comparison of various properties between all the Hetero Samples

	Sample	MgB ₂ layer Thickness (mm)	J _{c(zero)} (A/cm ²)	J _{c(3T)} (A/cm ²)	h _{max}	A _s	B _p	C _v
Single	Bi-2212	-	0.2 X10 ⁴	0.15x10 ⁴	0.33	1.56	0.46	2.38
Bi-Layer	Hetero-1	0.5	0.8 X10 ⁴	0.2 X10 ⁴	0.5	0.91	0.66	2.91
	Hetero-2	0.4	1 X10 ⁵	0.6 X10 ⁴	0.3	1.50	1.71	1.51
Tri-Layer	Hetero-3	0.7	1.9 X10 ⁵	0.8 X10 ³	0.29	2.87	3.88	3.76
	Hetero-4	0.6	2 X10 ⁵	0.1 X10 ⁴	0.2	4.20	3.85	1.92

CONCLUSIONS

Study the synthesis of Bi-2212 and MgB₂ heterostructures and their properties using various techniques. The superconducting phases of the prepared samples were confirmed with the help of X-ray diffraction patterns and DC magnetization characterizations. In the process of multilayer growth, it is observed that an inverted isotropy in the J_c. It may be due to the enhancement of ab-plane properties. STEM analysis of the samples illustrates the formation of the well-crystallised grains at surface cross sections. In heterostructures, the J_c has been increasing with respect to the superconducting volume fraction. It is also observed that the instability of the J_c for higher applied fields may be attributed to various pinning mechanisms and also variations in microstructures. The results suggest that the dominant pinning mechanism of a sample depends on the thickness of the heterostructure. The heterostructures of Bi-2212 and MgB₂ superconductors were synthesised and studied for their superconducting properties. Studies confirm the presence of both superconducting phases in these heterostructured samples.

Inverted anisotropy in J_c is may be due to enhancement of ab-plane properties in the multilayer growth process. The morphology of the samples at the surface cross-section shows well-crystallised grains of superconducting phases in their respective layers. J_c increases in the multilayer of Bi-2212 and MgB₂ superconductors due to an increase in superconducting volume fraction. Instability of J_c at high fields is attributed to different pinning mechanisms and microstructural variations in the samples. In the Hetero-1 sample, surface pinning due to grain boundaries is the dominant pinning mechanism. In Hetero-2 and Hetero-3 samples, point pinning due to lattice defects and impurities is the dominant pinning mechanism. In the case of a Hetero-4 sample, the volume pinning due to impurity phases is the dominant pinning mechanism.

ACKNOWLEDGMENTS

The authors are thankful to the University of Hyderabad, India for providing the facilities to characterize the samples.

REFERENCES AND NOTES

1. S. Lee, C. Tarantini, P. Gao et.al. Artificially engineered super lattices of pnictide superconductors, *Nat. Mater.* **2013**, 12, 392–396.
2. Y.T. Suga, H. Kurosaki, S.B. Kim et.al. YBa₂Cu₃O_{7-δ} deposition on Ni-Cr alloy tape by liquid phase epitaxy method, *Physica C*, **2002**, 378-381, 971-974.

3. A. Kiessling, J. Hanisch, T. Thersleff, et.al. Nanocolumns in YBa₂Cu₃O_{7-x}/BaZrO₃ quasi-multilayers: formation and influence on superconducting properties, *Supercond. Sci. Technol.*, **2011**, 24, 055018.
4. J. N. Eckstein, I. Bozovic, High-temperature superconducting multilayers and heterostructures grown by atomic layer-by-layer molecular beam epitaxy, *Annu. Rev. Mater. Sci.*, **1995**, 25, 679-709.
5. Triscone, J.-M., O. Brunner, L. Antognazza, A. D. Kent, and M. G. Karkut. YBa₂Cu₃O₇/PrBa₂Cu₃O₇ superlattices: Properties of Ultrathin superconducting layers separated by insulating layers, *Physical review letters*, **1990**, 64 (7), 804.
6. C.Z. Antoine et al., Characterization of Field Penetration in Superconducting Multilayers Samples, in IEEE Transactions on Applied Superconductivity, **2011**, 21(3), 2601-2604.
7. E. Zacharias, R. Singh. Crystallization and resistivity studies on Bi₄Sr₃Ca₃Cu_yO_x glasses. *Physica C: Superconductivity*, **1995**, 247(3-4), 221-230.
8. D.M. Gokhfeld, D.A. Balaev, M.I. Petrov, S.I. Popkov, K.A. Shaykhutdinov V.V. Val'kov, Magnetization asymmetry of type-II superconductors in high magnetic fields. *J. Appl. Phys.*, **2011**, 109, 033904.
9. D.X. Chen, R.B. Goldfab, R.W. Cross, A. Sanchez, Surface barrier and lower critical field in YBa₂Cu₃O_{7-δ} superconductors, *Physical Review B.*, **1993**, 48(8), 6426-6429.
10. D. Uthra, R.K. Singh. Fascinating current density features of noble metal doped YBa₂Cu₃O_{7-δ} (YBCO) Superconducting materials. *J. Integr. Sci. Technol.* **2019**, 7 (1), 10–13.
11. D.C. Larbalestier, L.D. Cooley, M.O. Rikel et al., Strongly linked current flow in polycrystalline forms of the superconductor MgB₂. *Nature*, **2001**, 410, 186-189.
12. C. Cheng, Y. Zhao, Significant improvement of flux pinning and irreversibility field of nano-Ho₂O₃ doped MgB₂. *Physica C*, **2007**, 463-465, 220-224.
13. V.G. Prokhorov et al, Flux pinning and the paramagnetic Meissner effect in MgB₂ with TiO₂ inclusions. *Supercond. Sci. Technol.*, **2009**, 22, 045027.
14. I. P. Rani, P. Saxena. Structural Characterization of Iron Doped Layered YBCO Superconductor. *J. Integr. Sci. Technol.* **2019**, 7 (1), 14–18.
15. D.X. Chen, R.W. Cross, A. Saenchez, Effects of critical current density, equilibrium magnetization and surface barrier on magnetization of high temperature superconductors. *Physica C*, **1993**, 33, 7, 695-703.
16. A.M. Campbell, J.E. Evetts. Flux vortices and transport currents in type II superconductors. *Adv. Phys.*, **1972**, 21, 199.
17. O. F. de Lima, C. A. Cardoso, Critical current density anisotropy of aligned MgB₂ crystallites. *Physica C*, **2003**, 386, 575-577.
18. D. Dew-Hughes, Flux pinning mechanisms in type II superconductors. *Philosophical Magazine*, **1974**, 30(2), 293-305.
19. E.J. Kramer, Scaling laws for flux pinning in hard superconductors. *J. Appl. Phys.*, **1973**, 44(3), 1360-1370.